

RV

Relaxation Voltammetry

RV - a method for the evaluation of barrier coatings

Introduction

Products made of steel have excellent mechanical properties. In addition, steel is an inexpensive material and therefore, iron in the form of steel is one of the most important technical raw materials of the daily life. Unfortunately, the chemical characteristics of steel are not so favorable. As a base metal, iron is sensitive to oxygen and humidity. As a consequence, unprotected steel corrodes very easily and the corrosion process does not only affect the optical appearance but also influences the mechanical properties unfavorably.

One way to protect corrosion sensitive materials is the application of organic coatings. The development of new coatings requires methods to optimize the formulation which have to be tested during their development by the coatings manufacturers. To obtain a ranking of the corrosion protective performance of new coating formulations, many different weathering tests are necessary. After the weathering, the degradation of the coating has to be evaluated using mainly mechanical tests or visual examination. These tests are time consuming and the degree of degradation has to be estimated. The need of an objective and relatively fast evaluation method is obvious. Here, electrochemical impedance spectroscopy (EIS) is widely used for the characterization as well as for the detection of defects of the coating. Moreover, this method is also applied for the determination of the water-uptake and the degree of blistering and delamination. EIS provides information about the mechanistic background of corrosion processes as well as detailed information about coating properties like capacitance C_C or coating/pore resistance R_C .

For the interpretation of EIS-data, physical models like equivalent circuits are required. The basic models are given in figure 1. Model A describes a realistic perfect 'barrier coating' with the coating capacitance C_C and the coating/pore resistance R_C . Model B represents the case of pores and defects in the coating with a second 'time-constant', which is correlated to the charge transfer, consisting of the charge transfer resistance R_{CT} and the double layer capacitor C_{DL} . This model is widely used in the literature.

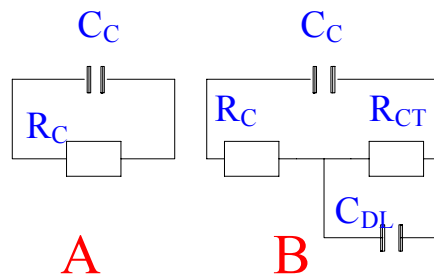


Fig. 1: Most popular basic equivalent circuits for the interpretation of the EIS spectra of organic coatings.

Unfortunately, the application of EIS in corrosion research shows some handicaps. For instance, commercially available 'barrier coatings' often show a low-frequency resistance around $10^{10} \Omega \cdot \text{cm}^{-2}$ or more. This requires a 'low frequency limit' of the measured spectrum in the mHz-region for the determination of R_C . Such measurements are rather time-consuming. They can easily exceed one hour.

Next, the measured system has to be in a steady state during the whole measuring time. Concerning water-uptake measurements for instance, it is save to assume that the constancy of the coating parameters (C_C and R_C) is not given in the early state of immersion. At least, considering the ratio of the number of measured specimens and the time required for a single measurement, a single impedance measurement seems to be rather time expensive.

In contrast to measurements of barrier coatings in the frequency domain, traditional methods in the time domain suffer from the special properties of this kind of systems. For instance, static DC-measurements enable the determination of R_C , but will not provide any information about dynamic parameters, neither about the dielectric properties nor about 'dynamic' processes (like diffusion contributions) within the coating. Dynamic measurements in the time domain which are reported in the literature [1,2], i. e. current interrupt techniques, suffer from the high resistances of the coating materials, too. On the one hand, so-called electrometers have an excellent accuracy in measuring current. However, these electronic devices are showing a poor resolution in time¹. Due to this fact, these instruments are not able to monitor (or to separate) fast processes. On the other hand, the current interrupt technique reported in the literature [2], delivers a resolution in measuring current of only 120 pA/digit. As will be shown below, this resolution is by far too low.

A relatively new technology for the investigation of high-Ohmic systems is the *Relaxation Voltammetry* (RV) [3-9]. This method is a current interrupt technique too, but it was designed especially to overcome the problems noted above. The principle of this technique is depicted schematically in figure 2 and explained in the following.

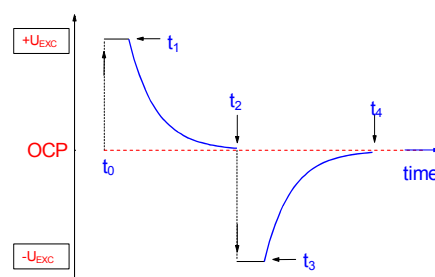


Fig. 2: The principle of RV

The potential $+U_{EXC}$ is superimposed to the open circuit potential (OCP) and causes a transient current (I_{EXC}) which tends to be constant after a certain time ($t_1 - t_0 = t_{EXC}$). After the current reaches this stationary state, it is switched off and the following decay of the potential $U(t)$ is recorded as a function of time (t_1 to t_2). The relaxation process is monitored using a sampling rate of 160 points per second (some 100 to some 1000 data points). After the potential reaches approximately the value of the OCP (at t_2 in figure 2), the procedure is repeated using the same excitation potential but with the opposite sign ($-U_{EXC}$).

Concerning the following considerations, the experimental procedure of RV differs essentially from 'traditional current interrupt techniques':

- 1.) In general, many electrochemical experiments are characterized by two parameters, potential and current. In potentiostatic mode of operation for instance, a potential is applied whereas the corresponding quantity (the current) is measured as a function of the actual potential. In contrast, in RV, a constant potential is applied and after interrupting the current, the potential is recorded as a function of the relaxation time. This kind of operation offers mainly two advantages. First of all, a potential in the range of 10^{-3} to 10^{-6} V can be measured more precisely than a current in the range of 10^{-12} to 10^{-15} A in principle. Besides this, the current (\pm) I_{EXC} is measured at its highest level, integrating over an interval (seconds) before the interrupt occurs, improving the accuracy additionally.
- 2.) Anodic **and** cathodic excitation are performed and both transients are measured. For the evaluation of the transient response $U(t)$, the values of both half-cycles are averaged, resulting in a 'symmetrical square-wave perturbation' around the OCP - similar to EIS.
- 3.) This 'symmetrical' operation is important, considering the experimental fact obtained from measurements of barrier coatings that the transients will not return exactly to the value of the OCP observed before the excitation. In a continuous mode of operation, t_{EXC} and/or U_{EXC} can be varied in subsequent cycles. Performing only anodic **or** cathodic excitation - like in 'traditional interrupt

¹ Usually, small currents are measured by integration a voltage drop at a shunt-resistor. But, the smaller the current the longer the time of integration for a given accuracy. As a consequence, the sampling rate of an electrometer is less than one point per second at the pA-level [7].

techniques' - would result in an irreversible shift² of the OCP. This would lead to erroneous results due to a superimposed (rest-) relaxation caused by the offset between the 'end-potential' (at t_2/t_4 in figure 2) and the OCP. To overcome this problem, in RV the OCP is 'updated' after each half-cycle from the values of the 'end-potential' of the actual and the latter half-cycle (for instance: $OCP = \frac{1}{2}(U_{t_4} + U_{t_2})$).

For sufficient accuracy the excitation time has to be chosen long enough to achieve settling. Figure 3 illustrates the influence of too short settling time on the voltage response. For a good compromise between time expense and available precision it is advisable to select the excitation time individually for a particular type of coating.

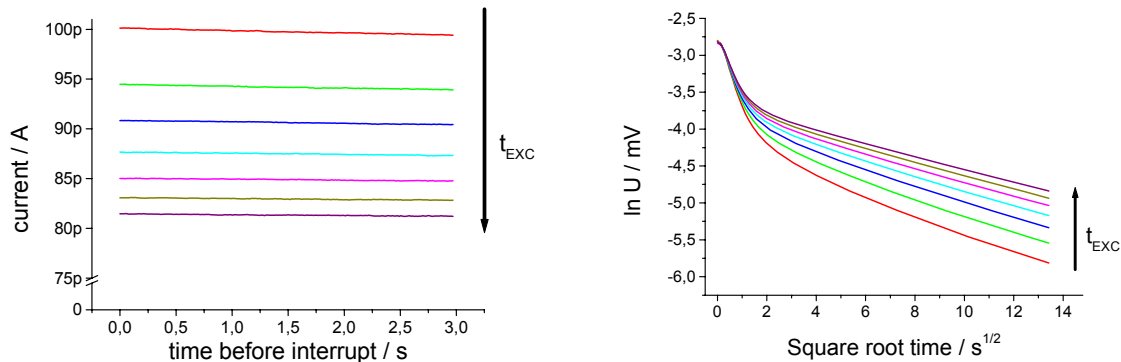


Fig. 3: Magnitude of the current before the interruption as a function of the excitation time t_{EXC} (left hand side) and the corresponding transients (right hand side). Scales are chosen for best visualization of the effect.

As one can see in figure 3 (left hand side), the current before the interruption decreases with increasing excitation time and settles to a constant value. The increased excitation time leads to a decrease in 'speed' of the corresponding transient, especially considering the long-time tail of the recorded voltage decay.

The applicability and performance of RV can be best represented by an example and in comparison to a measurement using EIS. In figure 4, the result of an RV measurement of a barrier coating is plotted as a function of the square root of the relaxation time (right diagram) whereas an impedance spectrum of the same specimen is shown at the left hand side of figure 4.

The DC accuracy of RV is best reflected regarding the small value of I_{EXC} ($1.33 \pm 0.01 \cdot 10^{-12}$ A), resulting from the total DC-resistance of the coating ($1.5 \cdot 10^{10} \Omega$ or $6.75 \cdot 10^{10} \Omega \cdot \text{cm}^{-2}$)³.

Comparing the results of EIS and RV in figure 4, the complementary nature of both techniques becomes aware. Considering the time (frequency) scale of both methods, one has to conclude that EIS handles the high frequency part (say above 1 Hz) accurately and without consuming too much time for the measurement. But at lower frequencies, the measuring time increases drastically which restricts the number of measured points (i. e. 5 points below 1 Hz in the above example) in practical measurements in a coating manufacturer's laboratory which may result either in a loss of accuracy or of information.

On the other hand, RV handles the middle and large relaxation range (above 1 second) which corresponds to the 'middle and low- frequency part' of an impedance spectrum very well. This fact is simply expressed by the number of measured points. A sufficient 'overlap' between the time scale of both methods arises from the initial sampling rate of RV which is shown in the following.

² A similar effect which is commonly observed in water-uptake measurements results from the drift of the OCP caused by the measured system itself.

³ Measuring area : 4.5 cm^2

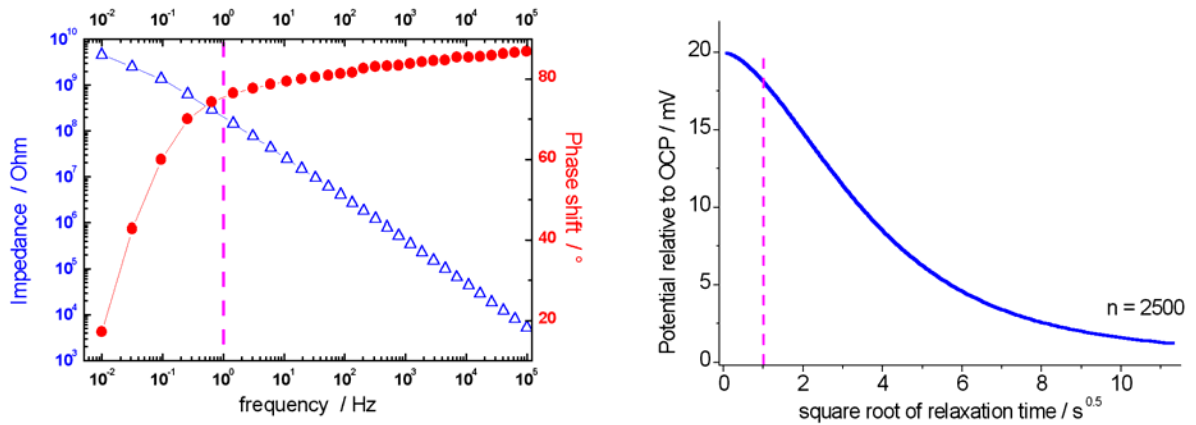


Fig.4 : RV and EIS as complementary techniques (see text)

In a comprehensive analysis of a huge number of different coating materials over a wide range of relaxation times it was found that the dielectric relaxation in barrier coatings can be explained by a hopping (random walk) process [10]. It is noteworthy that this so-called ‘two-step continuous time random walk’ (CTRW-2) exhibits a square root of time dependency of the corresponding time-law (equation 1) which seemed to contradict the results of EIS (see also [11,12]).

$$\phi(t) = \frac{U(t)}{U_{exc}} = \frac{1}{4^\beta - 1} \cdot \{ 4^\beta \cdot \exp[-(\lambda \cdot t)^\beta] - \exp[-(4 \cdot \lambda \cdot t)^\beta] \} \quad \text{Equation 1}$$

with $0 < \beta \leq 0.5$ and $\beta_{ideal} = 0.5$

However, in two publications [13,14] it was proven that there is no contradiction between the interpretation of the results of both techniques in principle, concerning the evaluated dielectric parameters.

Moreover, the evaluation of experimental data in frequency- and time domain according to the CTRW-2 process is now implemented into a commercial available software package. For this, two procedures have to be involved. On the one hand, time domain data have to be transformed into the frequency domain to evaluate the RV data with the techniques of EIS. The frequency transform is accomplished by a special kind of the discrete Fourier transform ‘Zoom Fast Fourier Transform’(ZFFT). A typical example is depicted in figure 5.

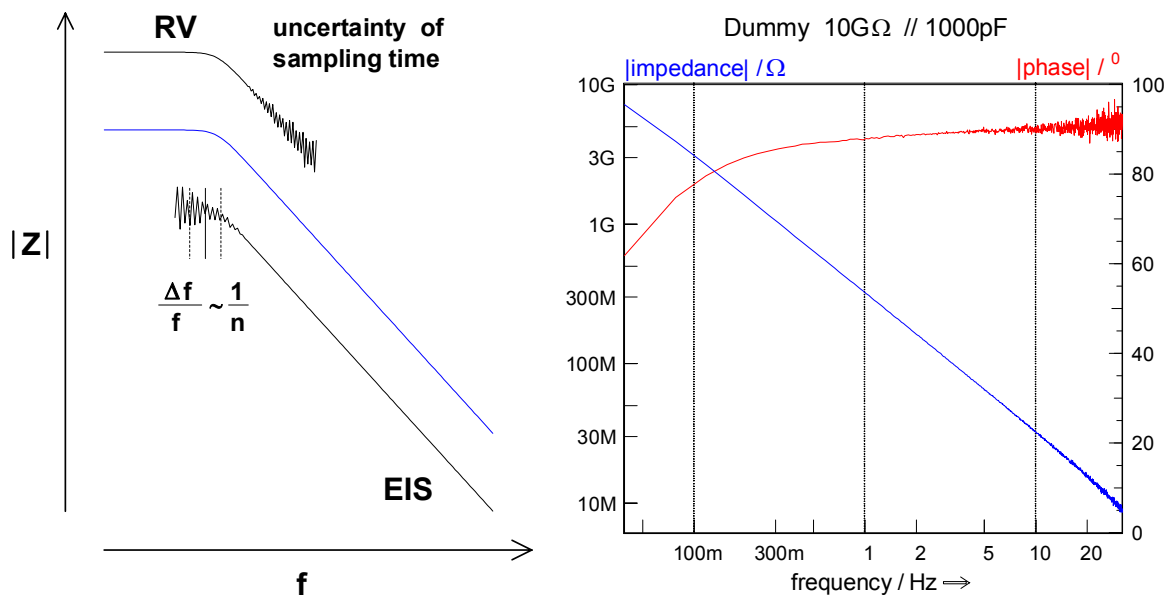


Fig. 5: Left hand side: 'complementary properties' of EIS and transformed RV data. Typical result of a frequency transformed RV transient (right hand side)

On the other hand, a numerical representation of the CTRW-2 process has been established to evaluate impedance data in the frequency domain according to this model. As noted above, the handling of experimental data in the frequency domain benefits from more simple mathematical operations, provided the transfer function of a distinct impedance element is known. Unfortunately, a closed analytical expression of the CTRW-2-function in the frequency domain does not exist. The transformation presented in the literature is a combination of numerical and analytical algorithms, designed for the evaluation of a sufficient wide range of frequencies which is convenient for the user. Further details are reported in the literature [15].

Summary

RV is a suitable tool for the investigation of high impedance systems. Although different applications can be seen, RV has been especially designed to meet the demands of the investigation of coated metals.

In contrast to 'traditional interrupt techniques', RV combines electrometer-type accuracy with an adequate resolution in time so that DC- as well as dielectric parameters of these systems are accessible. Both quantities are of great importance for the coatings manufacturer to improve their products. In comparison to EIS it is to state that both techniques supplement each other ideally. Undoubtedly, the big advantage of EIS for the evaluation of high impedance systems is the rapid determination of the dielectric properties whereas the strong points of RV are found to be in the 'middle and low frequency range'.

RV Hardware set-up

General

For Relaxation Voltammetry a high-sensitivity low-noise potentiostat is necessary. Although developed mainly for the measurement of Electrochemical Noise ECN, the Zahner Nprobe is well suited for RV purposes. The Thales RV script assumes, that a Nprobe is present and connected to the first inlet of a slave potentiostat extension of the IM6.

1. Connecting the Nprobe to the IM6

Use the thick black cable output of the Nprobe with the 8-pole Lemos plug and connect it to the input #1 of the IM6 EPC40 plug in card (figure 6). The device address of the Nprobe will then be registered as 1.

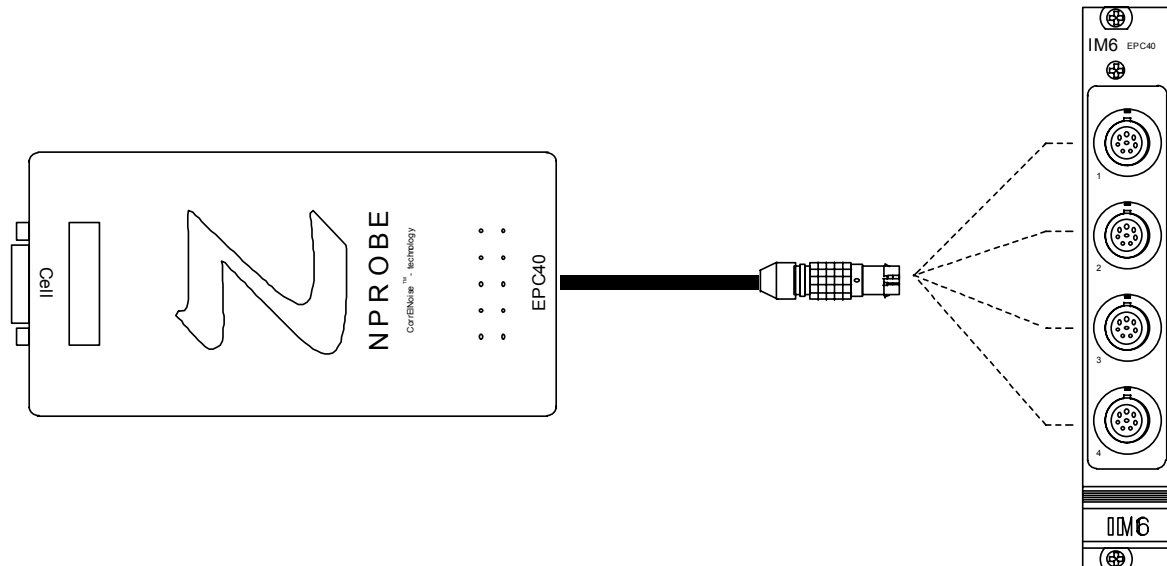


Fig. 6: The Nprobe to main instrument connection

2. Connecting the object under test

A special cable which supports both closed-loop ECN as well as RV measurements is attached to the Nprobe RV set-up (figure 7). Differing from the ECN arrangement, an additionally yellow marked inlet is used for the measurement of the potential. This inlet is designed for extreme low bias current necessary for RV.

Use the blue cable as current sense inlet of the working electrode, the yellow inlet for the reference electrode and the red outlet for the counter electrode. If you renounce on a dedicated reference electrode in a two-electrode set-up, connect the red and the yellow line together.

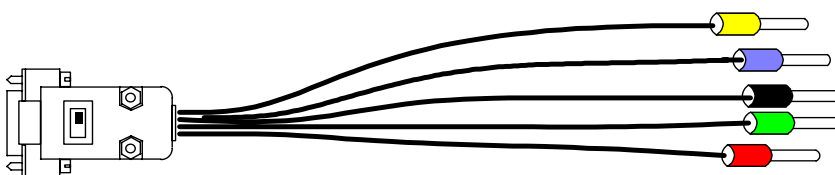
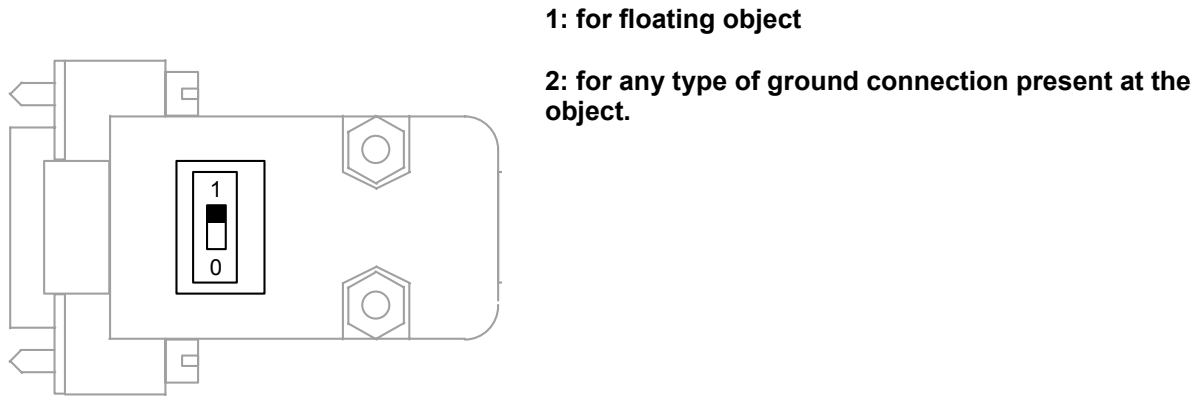


Fig. 7: The Nprobe sample connector

The black line should be connected to a surrounding Faraday cage. RV measurements are very sensitive to EMI. **It is very important to shield electromagnetic interference effectively !**

3. Select proper grounding conditions

Floating and ground referenced objects demand slightly different connections. Use the integrated switch in the 9-pin sub-D-plug to select (figure 8):



1: for floating object

2: for any type of ground connection present at the object.

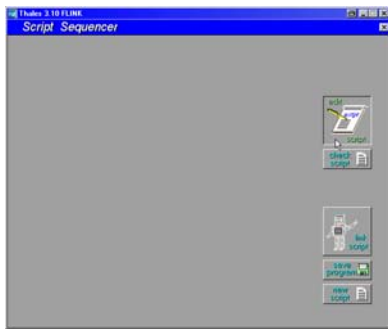
Fig. 8: Ground connector switch located on the sample connector cable plug at the Nprobe side.

RV Software Script Manual

4. How to enter RV

The functions of the Thales RV are provided in form of a script. Generally a script can be activated from the Thales desktop by pressing the “script”-button and performing the following procedure (figure 9):

Start
“script”
from the
Thales
desktop
script icon
The empty
script
menu
appears.



“edit script”



Open
source

„c:\thales\script\rv\rv.is_“



Return to the script panel and link the script



Fig. 9: How to open and compile a script source

Generally the source code is open for changes. However, we recommend this only to the experienced user. After successful linking the RV panel (figure 10) appears:

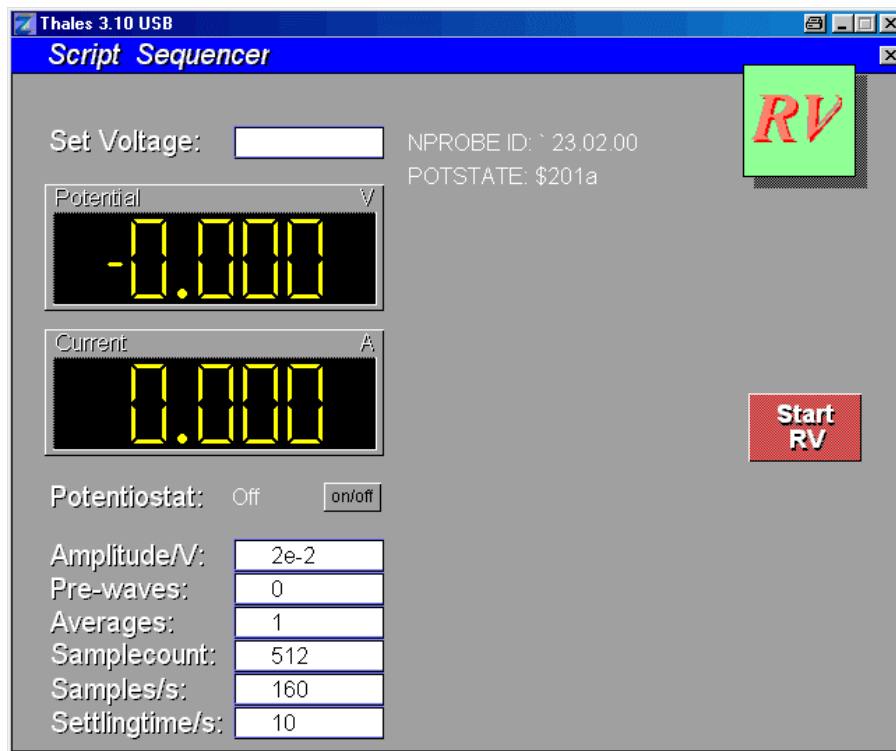


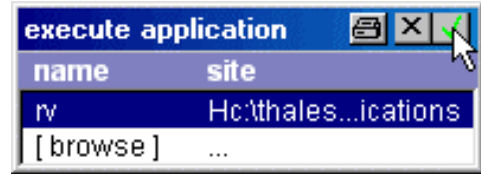
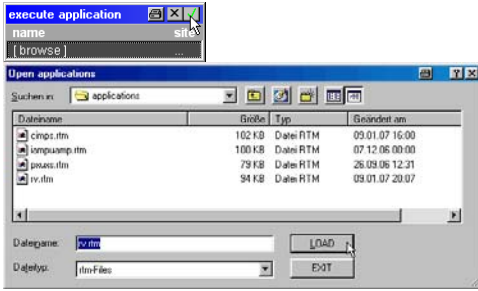
Fig. 10: RV script main menu

In the path "c:\thales\examples\applications" usually precompiled versions of script applications are present. Alternatively to the procedure described above, you can start RV like sketched in the following (figure 11):

enter "exe" from the Thales desktop



Use "browse" to find & start the program needed.

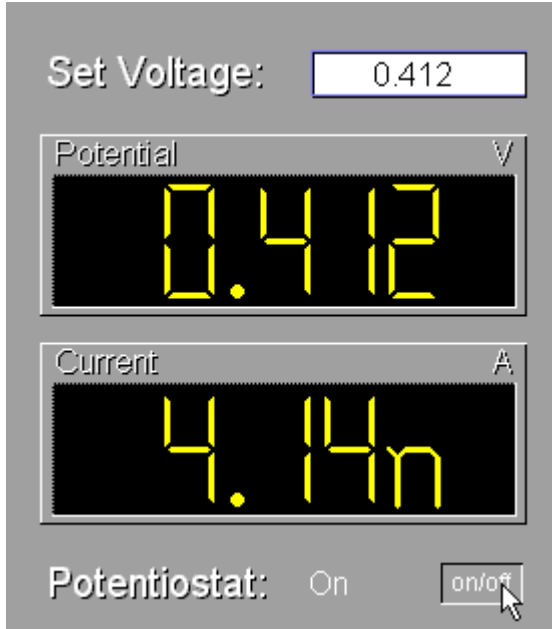


Re-enter by means of EXE, if necessary (right).

Fig. 11: Activating and re-entering a pre-compiled RV version by means of the EXE procedure

This procedure will save time. However, after exit of RV you will not find RV under the Thales desktop function "script". Instead you have to re-enter RV via the EXE function. Pre-compiled versions cannot be altered by the user.

5. Setting up measurement parameters



Once RV is active and the sample is connected, the display "Potential" will show the actual open circuit voltage of the cell. No (zero) current is displayed in this state.

If your sample does not exhibit a moderately stable open circuit potential, switch on the potentiostat and select a set voltage (figure 13) within the dynamic range of the Nprobe of ± 2.5 V close to the mean OC voltage.

It is also recommended to test the loop conditions by switching on the potentiostat like sketched in figure 12. Modify the set voltage slightly to check, if the measured potential follows the set value.

To perform RV, switch off again first !

Fig. 12: Display of the actual cell voltage and current, the toggle switch for the potentiostat state and the input field for the set voltage.

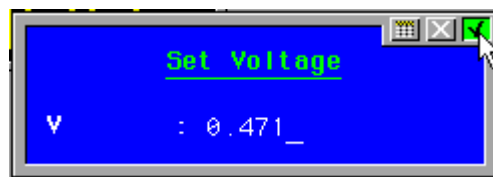
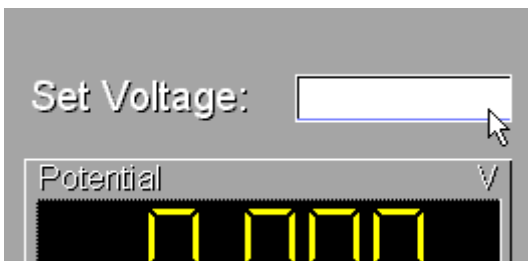


Fig. 13: A click on the input field for the set voltage will open the set voltage input box.

The measurement parameter set of RV is preset to values, which allow a fast “RV-shot”. Open and edit the parameters like sketched in figure 14, if you want to vary from the standard conditions.

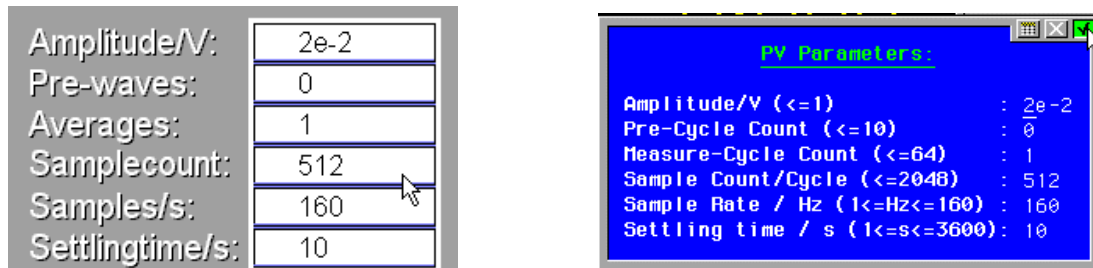


Fig. 14: A click on the input field for the RV parameters will open the parameter field input box.

Choose excitation amplitudes as a compromise between a minimal non-linearity and maximal signal-to-noise ratio. Values around 20mV are appropriate, but thick coatings may be tested also with higher amplitudes without problems, because the effective field strength responsible for non-linearity is much lower in this case.

Coatings exhibiting a stable electrochemistry can be studied without a pre-cycle to be discarded. For less stable coatings it is recommended to use at least one pre-cycle. The measure cycle count can be increased to increase the signal-to-noise ratio by means of averaging for the expense of longer measurement time.

The time window and resolution can be adjusted by means of the sample count per cycle and the sampling rate parameter. This parameters will determine also the frequency resolution (see chapter “Transform to EIS”).

Like discussed in the RV basics above, the excitation time (settling time, figure 2, 3 & 14) should be long enough to ensure a moderately stable excitation current. The useful range for the excitation time parameter depends strongly on the object under test.

6. Triggering an RV measurement

After setting up proper measurement conditions, an RV measurement is started by pressing the “start” button (figure 15).



Fig. 15: A click on “Start RV” will trigger an RV measurement according to the conditions selected.

The physical course of an RV was already described above in detail. The certain phases of RV – setting positive excitation – settling – relaxation - setting negative excitation – settling – relaxation - are visualized by certain graphics.

The excitation-settling phases are accompanied by numeric displays and progress bars (figure 16).

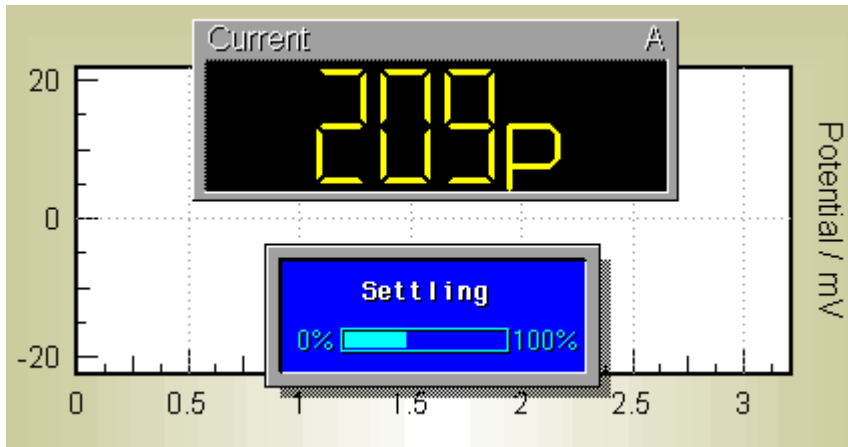


Fig. 16: RV starts with positive excitation. The actual current and the phase progress will be displayed.

potential. The course of the potential vs. time is displayed like shown in figure 17.

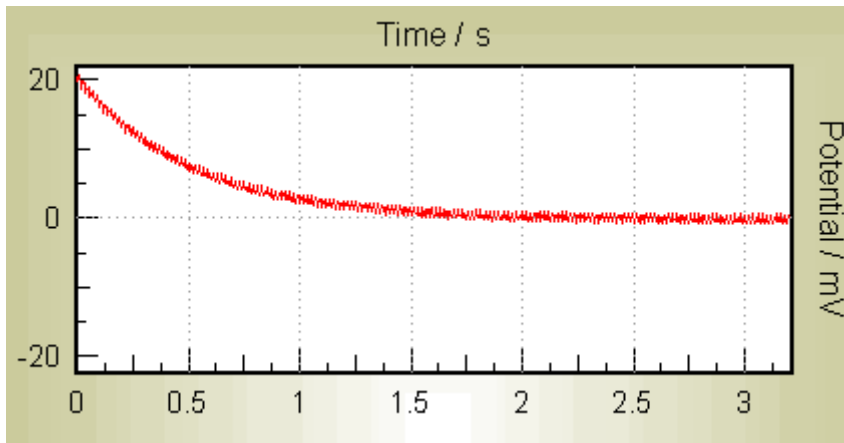


Fig. 17: Time course of the open circuit potential after positive excitation.

The positive phase is followed by the same sequence with negative sign.

After the completion of all pre- and measurement cycles, the time course of all relaxation phases will be displayed and the “RV completed”-menu appears (figure 18).

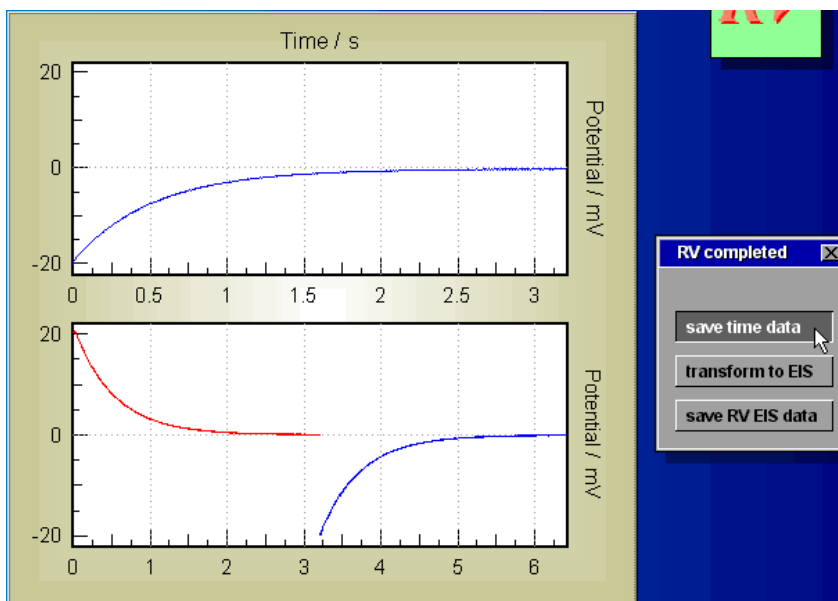


Fig. 18: Time course of the last relaxation (upper diagram) and of all RV phases after the completion of a measurement. The RV-end menu appears.

7. Data processing after an RV measurement

RV offers different options to save and process the data after a measurement. If you try to escape from the RV-end menu without saving the measurement results, an interrogation box appears (figure 19).



Fig. 19: Interrogation on escape, if unsaved data are present.

If you want to keep the time data, call "save time data" from the RV-end-menu (Fig.18 right hand side). An input box (figure 20 left) will offer you to comment the actual data set. The file manager opens then for saving the time domain data organized in form of the "pvi"-format. By means of the PVI-program RV-data may be opened and processed, for instance for the purpose of ASCII data list export.

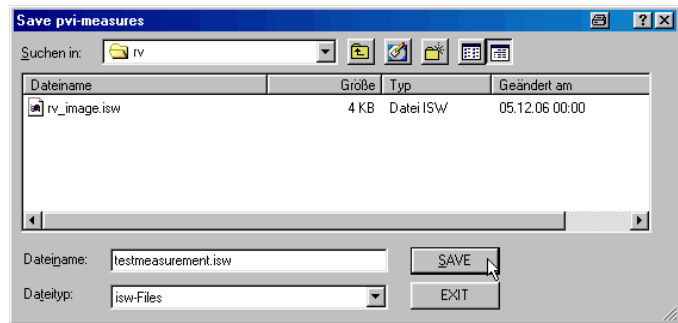
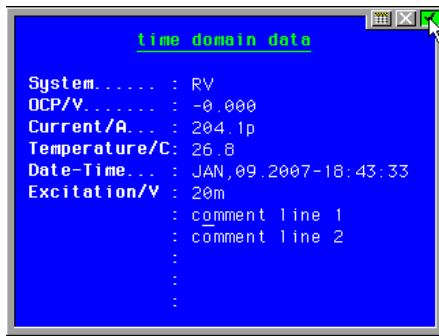
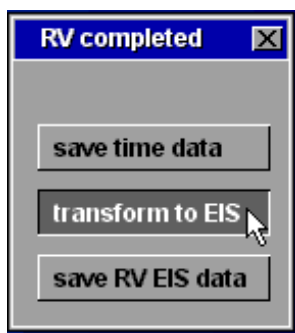


Fig. 20: Comment box for saving time domain data (left) and the corresponding file menu (right).

8. Transform RV data to EIS



Besides a direct analysis in the time domain, RV data may be processed advantageously in the frequency domain after transforming the measurement into EIS data. The impedance elements CTRW and CTRW2 can then be applied to the resulting spectra in the SIM environment. Choose "transform to EIS" from the RV-end-menu (figure 21).

The time domain data are treated "as if" periodically by means of a discrete Fourier transform (Zoom FFT), in spite of the fact, that they belong to single events. Consequently the corresponding EIS spectra are approximate. Figure 22 displays a typical result.

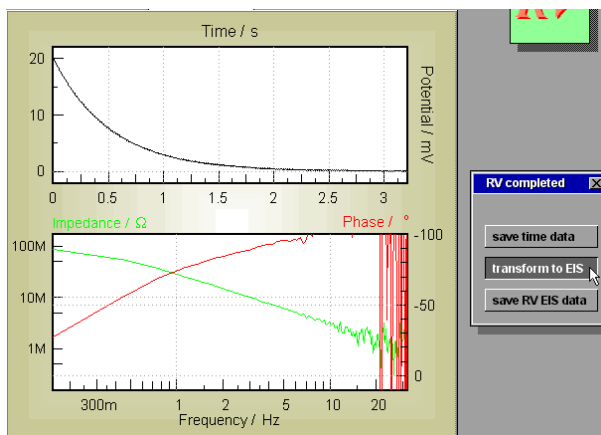


Fig. 22: A typical result of the transform operation from time domain data to EIS.

The EIS data may be stored similar to the time domain data (figure 20) for export and further analysis.

References

- [1] Granata, R. D.; Kovalski, K. J., 'Evaluation of High- Performance Protective Coatings by Electrochemical Impedance and Chronoamperometry' in 'Electrochemical Impedance : Analysis and Interpretation'; eds. : Scully, J. R.; Silverman, D. C.; Kendig, M. W.; ASTM STP 1188 (1993)
- [2] Tanabe, H.; Nagai, M.; Matsuno, H.; Kano; M.; 'Evaluation of protective coatings by a current interrupter technique' in 'Advances in Corrosion Protection by Organic Coatings II' (1994); ISBN 1-56677-108-0; pages 181 – 192; (from : *Materials and Corrosion* **47** (1996), abstract nr. 96-0831)
- [3] G. Meyer, H. Ochs, W. Strunz, J. Vogelsang; 'Barrier coatings with high Ohmic resistance - comparison between Relaxation Voltammetry and Impedance Spectroscopy'; Proceed. of EMCR 1997, 25. - 29. -8. 1997, Trento Italy, oral contribution
- [4] G. Meyer, H. Ochs, W. Strunz, J. Vogelsang; *Materials Science Forum*, 289-292 (1998) 305
- [5] H. Ochs, W. Strunz, J. Vogelsang; 'Relaxation voltammetry with organic barrier coatings on steel - experimental and theoretical approach'; Proceed. of EMCR 1997, Trento, Italy, poster presentation
- [6] G. Meyer, H. Ochs, W. Strunz, J. Vogelsang; *Materials Science Forum*, 289-292 (1998) 373
- [7] W. Strunz, J. Vogelsang; 'Characterization and evaluation of organic coatings using relaxation voltammetry'; Proceed. of EUROCORR 1998, Utrecht, Netherlands, oral contribution
- [8] J. Vogelsang, W. Strunz; 'Barrier coatings - a challenge for EIS and RV'; Proceed. of EIS 1998, Rio de Janeiro (Brasil).
- [9] J. Vogelsang, U. Eschmann; G. Meyer, W. Strunz; *Farbe & Lack* **104**:5 (1998) 28.
- [10] W. Strunz; *Prog. Org. Coat.* **39** (2000) 49
- [11] J. Vogelsang, W. Strunz; *Materials and Corrosion* **52**:6 (2000) 462.
- [12] J. Vogelsang, W. Strunz; *El. Acta* 46 (2001) 3817
- [13] C. A. Schiller, W. Strunz; *El. Acta* 46 (2001) 3619
- [14] W. Strunz; 'The frequency behavior of the 'two-step' continuous time random walk'; Proceed. of EMCR 2000, Budapest, Hungary, oral contribution (200[15] W. Strunz, C. A. Schiller, J. Vogelsang; *El. Acta* 51 (2006) 1437